Bacteria modulate tamoxifen-induced death via host fatty acid metabolism

Cédric Diot[1], Aurian P. García-González[1], Andre F. Vieira[2], Melissa Walker[1], Megan Honeywell[1], Hailey Doyle[1], Yomari Rivera[1], Huimin Na[1], Hefei Zhang[1], Michael Lee[1], Carissa P. Olsen[2], Albertha J.M. Walhout[1*]

[1]Department of Systems Biology, University of Massachusetts Chan Medical School, Worcester, MA, 01605, USA

[2]Department of Chemistry and Biochemistry, Worcester Polytechnic Institute, 100 Institute Road, Worcester, MA, 01609, USA

*Lead contact: marian.walhout@umassmed.edu

SUMMARY

Tamoxifen is a selective estrogen receptor (ER) modulator that is used to treat ER-positive breast cancer, but that at high doses kills both ER-positive and ER-negative breast cancer cells. We recapitulate this off-target effect in *Caenorhabditis elegans*, which does not have an ER ortholog. We find that different bacteria dramatically modulate tamoxifen toxicity in *C. elegans*, with a three-order of magnitude difference between animals fed *Escherichia coli*, *Comamonas aquatica*, and *Bacillus subtilis*. Remarkably, host fatty acid (FA) biosynthesis mitigates tamoxifen toxicity, and different bacteria provide the animal with different FAs, resulting in distinct FA profiles. Surprisingly these bacteria modulate tamoxifen toxicity by different death mechanisms, some of which are modulated by FA supplementation and others by antioxidants. Together, this work reveals a complex interplay between microbiota, FA metabolism and tamoxifen toxicity that may provide a blueprint for similar studies in more complex mammals.

31 **INTRODUCTION**

32 The bacteria that inhabit our body, known as our microbiota, influence many biological
33 processes in both health and disease, and greatly contribute to our metabolic capacity
34 (Koppel et al., 2017; Spanogiannopoulos et al., 2016). The bacteria from the gut
35 microbiota are among the first cells to encounter orally ingested nutrients and xenobiotics.
36 Therefore, it is perhaps not surprising that the microbiota can also impact our response
37 to medications (Koppel et al., 2017). Several mechanisms have been identified by which
38 microbes influence the host's drug response. First, the microbial composition can change
39 in response to drugs. Known as dysbiosis, such altered composition can affect the host's
40 response to therapeutic drugs (Diot et al., 2018; Maier et al., 2018). Second, bacteria can
41 alter host drug availability, for instance by drug sequestration or modification (Koppel et
42 al., 2017; Zhang et al., 2021). Third, the metabolic crosstalk between the microbiota and
43 its host can modify host physiology, and consequently drug efficacy (Selwyn et al., 2015).
44 All these processes can change drug action and it is therefore important to systematically
45 identify which bacteria modulate the efficacies of which drugs, and to dissect the
46 mechanisms involved.

47 Systematic identification of microbial effects on the host's drug response in
48 humans or mammalian model systems is challenging because of their complex diet and
49 microbiota, as well as relatively low scalability. Recently, we and others, have developed
50 the nematode *Caenorhabditis elegans* and its bacterial diet as an interspecies model
51 system to rapidly assess the animal's response to different drugs and how this response
52 can be modulated by different bacteria (Garcia-Gonzalez et al., 2017)(Rosener et al.,
53 2020; Scott et al., 2017). The application of high-throughput genetic screens not only in

54 the host, but also in the bacteria it consumes, make this a powerful model (Diot et al.,
55 2018; Garcia-Gonzalez and Walhout, 2017; Watson et al., 2013; Watson et al., 2014).
56 Recent studies illustrate the insights on host-bacteria-drug interactions that can be
57 obtained using this model system. In a screen with 11 chemotherapeutic drugs and two
58 bacterial diets, we found that three drugs, 5-fluoro-2'-deoxyuridine (FUDR), 5-fluoro-uracil
59 (5-FU) and camptothecin (CPT) elicited a reproductive phenotype, two of which were
60 modulated by the two bacteria, in opposite directions (Garcia-Gonzalez et al., 2017).
61 Specifically, a diet of *Escherichia coli* rendered the animals more sensitive to FUDR, but
62 less sensitive to CPT, relative to a diet of *Comamonas aquatica* (Garcia-Gonzalez et al.,
63 2017). We found that bacterial pyrimidine metabolism, specifically the generation of 5-
64 fluorouridine monophosphate (FUMP), was critical to FUDR toxicity in the animal (Garcia-
65 Gonzalez et al., 2017; Scott et al., 2017).

66 Tamoxifen is a triphenylethylene belonging to the class of drugs known as
67 selective estrogen receptor modulators (SERMs). SERMs bind to and either activate or
68 repress the estrogen receptor (ER), a nuclear hormone receptor (NHR) transcription
69 factor (Shelly et al., 2008). Tamoxifen is commonly used to treat ER-positive breast
70 cancers, as well as other estrogen-dependent ailments such as ovarian or endometrial
71 carcinoma (Jordan, 2003; Shagufta and Ahmad, 2018). A significant proportion of ER-
72 negative breast cancers also appear responsive to tamoxifen, but the underlying biology
73 remains to be uncovered (Manna and Holz, 2016). There has also been increasing clinical
74 interest in the potential of tamoxifen for treating various other cancer types (Clifford et al.,
75 2020). The potential repurposing of tamoxifen for the treatment of non-ER-positive breast

76 malignancies requires an understanding of the potential alternative mechanisms of action
77 of this drug, especially in ER-negative models.
78 The *C. elegans* genome encodes more than 250 NHRs (Reece-Hoyes et al.,
79 2005). Most of these are paralogs of HNF4α and there is no ER ortholog. We find that
80 tamoxifen is toxic in *C. elegans* at higher doses and that three bacterial species, *E. coli,*
81 *C. aquatica,* and *Bacillus subtilis,* confer dramatically different levels of sensitivity to
82 tamoxifen toxicity, with an EC_{50} ranging three orders of magnitude. We identify a role for
83 host fatty acid (FA) metabolism in modulating tamoxifen toxicity. We further find that the
84 FA composition of *C. elegans* is greatly modulated by bacterial diet. Most strikingly, we
85 find that different bacteria modulate *C. elegans* tamoxifen toxicity through different death
86 mechanisms. Taken together, we show that a complex interplay between bacteria, FA
87 metabolism and different mechanisms of death modulate tamoxifen toxicity in *C. elegans*.
88
89 **RESULTS**
90
91 **Tamoxifen Kills both ER-Positive and ER-Negative Cancer Cells**
92 We first confirmed that tamoxifen can kill ER-negative breast cancer cells (Bekele et al.,
93 2016). Specifically, we compared the effects of tamoxifen on ER-positive T-47D cells,
94 which rely on ER for proliferation, to the effects of tamoxifen on ER-negative MDA-MB-
95 231 cells (Lacroix and Leclercq, 2004). Drug toxicity can be assessed through two
96 parameters: growth rate and fractional viability. The growth rate (GR) index is calculated
97 by the relative number of live cells over time in presence or absence of drug and
98 integrates both cytostatic and lethal effects of a drug (Hafner et al., 2016). In contrast,

99 fractional viability only considers the lethal effect of a drug (Schwartz et al., 2020). We
100 first calculated the GR index and, as expected, observed a decrease in the growth rate
101 of T-47D cells incubated with tamoxifen in a dose-dependent manner (**Figure 1A**). While
102 lower doses of tamoxifen did not affect the growth rate of MDA-MB-231 cells, we found
103 that concentrations greater than 10 μM resulted in a reduction in the population growth
104 rate, indicating either a reduced cell proliferation rate or increased cell death rate
105 (**Figure 1A**). When we computed fractional viability, we found that a dose of tamoxifen
106 greater than 10 μM, killed both T-47D and MDA-MB-231 cells effectively (**Figure 1B**).
107 This indicates that tamoxifen toxicity relies on two distinct mechanisms depending on the
108 dose: at low doses, tamoxifen slows the growth of ER-positive, but not ER-negative cells,
109 whereas at high doses, tamoxifen kills independently of whether the cells express ER.
110 Since this cell death does not depend on ER, it can be considered an off-target effect.
111

112 **Bacteria Differentially Modulate Tamoxifen Toxicity in *C. elegans***

113 *C. elegans* does not have an obvious ER ortholog (Reece-Hoyes et al., 2005; Taubert et
114 al., 2011). Therefore, we wondered whether we could use *C. elegans* to study off-target
115 tamoxifen toxicity in an intact animal. Since we previously found that the bacterial diet
116 consumed by *C. elegans* can greatly affect the response to chemotherapeutic drugs
117 (Garcia-Gonzalez et al., 2017), we supplemented increasing doses of tamoxifen to
118 animals fed either of three different bacterial diets: *E. coli, C. aquatica* or *B. subtilis*. Visual
119 inspection showed dramatic differences in tamoxifen toxicity, depending on bacterial
120 diet: there was little effect on animal development on *E. coli*, while animals fed *C. aquatica*
121 displayed developmental arrest or delay at high drug concentrations, and animals fed

122 *B. subtilis* were exquisitely sensitive to tamoxifen, even at low micromolar concentrations
123 (**Figure 1C**). We observed many arrested first larval stage (L1) animals in the presence
124 of high concentrations of tamoxifen, and therefore quantified tamoxifen toxicity by
125 counting the proportion of animals that failed to develop at different doses of the drug.
126 The resulting dose response curves (DRCs) confirmed that tamoxifen is more than three
127 orders of magnitude more toxic to animals fed *B. subtilis* than to animals fed *E. coli*
128 (**Figure 1D**). Together, these results show that tamoxifen is toxic to *C. elegans* at high
129 doses and that bacteria greatly modulate this toxicity.
130

131 ***C. elegans* Fatty Acid Synthesis Protects Against Tamoxifen Toxicity**

132 When fed *E. coli*, tamoxifen is only toxic to *C. elegans* at high micromolar doses (**Figure**
133 **1D**). We hypothesized that *C. elegans* metabolism may modulate tamoxifen toxicity.
134 Therefore, we screened an RNAi library of 1,495 *C. elegans* metabolic genes (in *E. coli*)
135 for increased or decreased drug toxicity. This library includes genes with known metabolic
136 functions that make up the genome-scale iCEL1314 metabolic network model, as well as
137 other genes that are predicted to encode metabolic enzymes (Yilmaz et al., 2020; Yilmaz
138 and Walhout, 2016). We did not find any genes that, upon RNAi knockdown, rendered
139 the animals less sensitive to tamoxifen. We did, however, identify three genes for which
140 RNAi knockdown led to increased tamoxifen toxicity (**Figure 2A**). These genes include
141 *dhs-19*, which encodes a short-chain dehydrogenase of unknown function that localizes
142 to lipid droplets (Liu et al., 2018) and is predicted to function in retinol metabolism (Yilmaz
143 et al., 2020). The other two genes, *elo-3* and *elo-6,* both encode elongases predicted to
144 be involved in long chain FA biosynthesis (Walker et al., 2021; Watts, 2009). We

145 generated a *dhs-19* deletion mutant by CRISPR/Cas9 genome editing and confirmed that
146 this strain is more sensitive to tamoxifen (**Figure 2B**, **Figure S1**).

147 While mutant strains are available for *elo-3* and *elo-6*, we could not use these
148 animals because their development is strongly impaired even in absence of drug
149 exposure (data not shown). Both *elo-3* and *elo-6* function in FA biosynthesis (**Figure 2C**).
150 We wondered if these two genes specifically affect tamoxifen toxicity, or if FA metabolism
151 is more broadly involved even though no other genes were captured in the RNAi screen.
152 To test this, we performed full tamoxifen DRC experiments for the knockdown of 33 genes
153 encoding enzymes predicted to be involved in FA elongation and desaturation (Walker et
154 al., 2021)(**Figure 2C**). In addition, we included eight genes encoding acyl-CoA
155 synthetases that catalyze the addition of co-enzyme A (CoA) to FAs and eight genes
156 encoding enzymes that remove CoA. We calculated the difference between the area
157 under the curve (ΔAUC) for each RNAi condition + tamoxifen relative to *E. coli* (**Figure**
158 **2D**). Statistical significance was evaluated on the original DRCs (**Figure S2, Tables S1**
159 **and S2**). Remarkably, knockdown of most FA biosynthesis genes tested significantly
160 increased tamoxifen toxicity (**Figure 2E, Figure S2, Table S1**). These results show that
161 *C. elegans* FA synthesis is broadly involved in mitigating tamoxifen toxicity. This points to
162 a systems-level involvement of FA biosynthesis rather than a single FA species.

163 Next, we asked whether genes involved in mitochondrial and peroxisomal FA
164 degradation also modulate tamoxifen toxicity and found that, of 33 genes tested, only
165 *ech-8* appeared to increase tamoxifen toxicity, but this effect was not statistically
166 significant (**Figure 2F, Figure S3**). Knockdown of 13 of the 33 FA degradation genes
167 tested led to a decrease in tamoxifen toxicity, with only *daf-22* RNAi being statistically

168 significant (**Table S2**). This result shows that the biosynthesis, but not degradation, of
169 long chain FAs is critical to mitigate tamoxifen toxicity in *C. elegans.*
170
171 **Bacterial Diets Modulate *C. elegans* Fatty Acid Profiles**
172 Previously, it has been shown that different strains of *E. coli* diets affect the FA
173 composition of *C. elegans* (Brooks et al., 2009). Since *C. elegans* FA synthesis modulates
174 tamoxifen toxicity, we hypothesized that the three bacterial species used herein may elicit
175 different FA profiles in the animal. To test this, we measured both bacterial and *C. elegans*
176 FA profiles by gas chromatography-mass spectrometry (GC-MS) (**Table S3** and **S4**). The
177 bacterial FA profiles showed dramatic differences: *E. coli* mainly contained the saturated
178 FAs (SFAs) palmitic acid and stearic acid, cyclopropane FAs (CPFAs), and the mono-
179 unsaturated FAs (MUFAs) oleic acid, palmitoleic acid and cis-vaccenic acid; *C. aquatica*
180 mainly contained the MUFAs oleic acid and palmitoleic acid; and *B. subtilis* almost
181 exclusively contains monomethyl branched chain FAs (mmBCFAs), which agrees with
182 previous findings (Kaneda, 1977) (**Figure 3A**).
183 The FA profiles of *C. elegans* fed the three bacteria reflected the three bacterial
184 diets in some but not all respects. One striking observation was that the proportion of
185 each of the different poly-unsaturated FAs (PUFAs) is diet-independent (**Figure 3B**). This
186 indicates that the animal can effectively convert different dietary FAs into PUFAs by
187 elongation and/or desaturation. Oleic acid is the primary substrate for PUFA synthesis
188 and is present in *E. coli* and *C. aquatica* but absent in *B. subtilis* (**Figure 3A**). This could
189 indicate that PUFAs are generated by a combination of FA metabolic steps that yield this

190 even-chained MUFA from odd-chained mmBCFAs in animals fed *B. subtilis* or
191 synthesizes them de novo.

192 Another striking observation is that most other types of FAs are quite different in
193 proportion in *C. elegans* fed different bacterial diets. Most notable are the near absence
194 of MUFAs, and presence of C15 and C17-ante-iso mmBCFAs in animals fed *B. subtilis*
195 (**Figure 3B**). The differences between animals fed the other two bacteria are more subtle,
196 with a greater proportion of the MUFA cis-vaccenic acid in *C. aquatica*-fed animals,
197 relative to those fed *E. coli* (**Figure 3B**). Altogether, the different bacterial diets result in
198 a different proportion of the different types of FAs: high overall levels of MUFAs in animals
199 fed *E. coli* or *C. aquatica* and high overall levels of mmBCFAs in animals fed *B. subtilis*
200 (**Figure 3B**, bottom). Taken together, these results show that *C. elegans* maintains its
201 PUFA content in a narrow and well-defined regime, while it can tolerate different
202 proportions of the other types of FAs.

203

204 **Dietary Fatty Acids Modulate Tamoxifen Toxicity**

205 Our findings so far lead us to consider two models: either tamoxifen treatment could alter
206 the animal's FA profile, leading to diet-dependent toxicity, or differences in *C. elegans* FA
207 composition elicited by bacterial diet may modulate tamoxifen toxicity. To discriminate
208 between these two models, we first measured bacterial and *C. elegans* FAs in the
209 presence or absence of tamoxifen and found that the drug did not modulate the animal's
210 FA profiles (**Table S5**). Thus, we did not find evidence to support the first model.

211 To evaluate the second model, we first asked whether supplementation of a FA
212 cocktail, containing equimolar amounts of the PUFAs arachidonic and linoleic acid, the

213 SFAs lauric and myristic acid, and the MUFA oleic acid (Sharma et al., 2013), would
214 modulate tamoxifen toxicity in animals fed either of the three bacterial diets. We found
215 that FA cocktail supplementation suppressed tamoxifen toxicity but only in animals fed *C.*
216 *aquatica*; it had no effect on tamoxifen toxicity in animals fed *E. coli* or *B. subtilis* (**Figure**
217 **4A-C**). Next, we tested the effects of the supplementation of individual FAs and found
218 that MUFAs such as cis-vaccenic acid increased tamoxifen toxicity on animals fed *E. coli*,
219 but not *C. aquatica* (**Figure 4D and 4E, Figure S5**). Since *C. aquatica*-fed animals contain
220 more cis-vaccenic acid than *E. coli*-fed animals (33% vs 20%, **Figure 3B**), this suggests
221 that this difference may contribute to increased tamoxifen toxicity on the *C. aquatica* diet.
222 Supplementation of individual PUFAs such as α-linoleic acid decreased tamoxifen
223 toxicity on animals fed *C. aquatica*, (**Figure 4F and 4G, Figure S5**). On an *E. coli* diet
224 PUFAs had no effect. However, animals are generally tolerant to tamoxifen, which limits
225 the ability to observe decreased tamoxifen toxicity. Since the proportion of PUFAs is
226 similar in animals fed each of the three bacterial diets (**Figure 3B**), this indicates that the
227 ratio of PUFAs to other FAs is more relevant than absolute levels. Surprisingly,
228 supplementation of either MUFAs or PUFAs abolished the growth of *B. subtilis*, and
229 therefore these FA could not be tested for tamoxifen toxicity modulation in *C. elegans* fed
230 these bacteria (**Figure 4H and 4I**). Together with the observation that knockdown of
231 genes involved in FA synthesis increases tamoxifen toxicity, these results point to a
232 complex interplay between dietary FA, FA synthesis and tamoxifen toxicity.
233 The FA cocktail is stabilized by vitamin E, a potent antioxidant that inhibits FA
234 oxidation (Traber and Atkinson, 2007). Therefore, we performed a control experiment by
235 supplementing only vitamin E. We found that vitamin E had no effect on tamoxifen toxicity

236 in animals fed either *E. coli* or *C. aquatica*, indicating that it is the FAs in the FA cocktail
237 that mitigate toxicity in animals fed *C. aquatica*. To our surprise, we found that vitamin E
238 supplementation did suppress tamoxifen toxicity in animals fed *B. subtilis* (**Figure 4J-L**).
239 However, N-acetylcysteine, another antioxidant that can rescue the growth of *C. elegans*
240 on iron-deficient *E. coli* mutants (Zhang et al., 2019) did not affect tamoxifen toxicity
241 (**Figure 4M**). These results indicate that FA oxidation, but not the general accumulation
242 of reactive oxygen species (ROS), affects tamoxifen toxicity in *C. elegans* when fed *B.*
243 *subtilis*. Since FAs rapidly turnover in the animal's membranes (Dancy et al., 2015), the
244 observation that FA biosynthesis mitigates tamoxifen toxicity (**Figure 2E**) could be
245 explained because it replenishes oxidized FAs.
246 Taken together, these results indicate that FA or vitamin E supplementation can
247 mitigate tamoxifen toxicity differently depending on which bacteria the animals are fed,
248 which suggests that different, diet-dependent toxicity mechanisms are involved.
249
250 **Bacteria Elicit Different Tamoxifen-Induced Death Mechanisms**
251 Lipid metabolism has been linked to different mechanisms of cell death, especially
252 apoptosis and ferroptosis (Galluzzi et al., 2018; Garbarino and Sturley, 2009). In fact, it
253 has been shown that cell survival is dependent on lipid homeostasis, and both excessive
254 MUFAs or SFAs have been shown to be pro-apoptotic, depending on the cell lines
255 (Garbarino and Sturley, 2009). Further, several MUFAs have been reported to protect
256 against ferroptosis (Magtanong et al., 2019), which is characterized by lipid peroxidation,
257 while others, specifically cis-vaccenic acid have been reported to induce cell death
258 (Nakamura et al., 2018). PUFAs, most notably di-homo-gamma-linoleic acid, have been

259 shown to induce ferroptosis in both human cells and in *C. elegans* (Perez et al., 2020).
260 Given these connections, we asked whether apoptosis contributes to tamoxifen toxicity
261 in *C. elegans*. To test this, we used *ced-3(n717)* mutant animals that cannot execute
262 apoptosis, because they harbor a substitution in the acceptor splice site of exon 7
263 encoding for the caspase p10 domain of the CED-3 protein (Yuan et al., 1993).

264 Remarkably, loss of *ced-3* greatly increased sensitivity to tamoxifen in animals fed
265 either *E. coli* or *C. aquatica* but had no effect on animals fed *B. subtilis* (**Figure 5A-C**).
266 This result suggests that, when fed *E. coli* or *C. aquatica,* tamoxifen toxicity employs
267 apoptosis, and that *ced-3* mutant animals switch to another, more potent mode of death
268 that is suppressed when apoptosis is functional. We additionally observed that a high
269 dose of vitamin E could mitigate tamoxifen toxicity in *ced-3* mutant animals fed *C. aquatica*
270 but not *E. coli* (**Figure 5A and 5B)***.* This indicates that, in the absence of *ced-3*, tamoxifen
271 toxicity in animals fed *C. aquatica* involves FA oxidation, similar to what we observed with
272 wild type animals fed *B. subtilis*.

273 Finally, we used expression profiling by RNA-seq to ask whether tamoxifen
274 supplementation results in the modulating the expression of genes involved in FA
275 metabolism or oxidative stress in *C. elegans*. As discussed above, tamoxifen does not
276 affect the animal's FA profiles and accordingly, the expression of FA biosynthesis or
277 degradation genes was not systematically altered upon tamoxifen exposure, with the
278 exception of *fat-5* which showed a three-fold increase, and *ech-6* which was reduced
279 by ~two-fold (**Figure 5D**). We did, however identify increased expression of R05D8.9
280 (**Figure 5D**), which encodes a predicted 17beta-hydroxysteroid dehydrogenase 14
281 (17βHSD14) homolog. In humans, 17βHSD14 enzymes are associated with the response

282 to tamoxifen in breast cancer (Sivik et al., 2012). These enzymes are further known to
283 interconvert different steroids, suggesting that R05D8.9 may be directly involved in the
284 detoxification of tamoxifen in *C. elegans*. In addition, the expression of several CYP
285 genes, which encode cytochrome P450 enzymes, is induced by tamoxifen
286 supplementation (**Figure 5D**). Cytochrome P450 enzymes have been reported to modify
287 tamoxifen in humans (Singh et al., 2011), and are a source of oxidative stress as their
288 enzymatic cycle involves significant leakage of electrons (Hrycay and Bandiera, 2015).
289 Taken together, tamoxifen does not transcriptionally rewire FA metabolism. In contrast, it
290 induces the expression of ROS-generating detoxifying enzymes, that may contribute to
291 FA oxidation.
292
293 **DISCUSSION**
294
295 **Tamoxifen Off-Target Mechanisms: Fat Metabolism, Oxidative Stress and**
296 **Microbiota**
297 In this study, we present *C. elegans* as a model to study off-target, ER-independent,
298 mechanisms of tamoxifen toxicity using concentrations in the range of drug-levels
299 accumulating in patients (Kisanga et al., 2004; Robinson et al., 1991). We found that FA
300 biosynthesis and composition of the animals are major drivers of tamoxifen toxicity, and
301 that this toxicity relies on the potential of the drug to induce oxidative stress and lipid
302 peroxidation. Moreover, we found that both the mechanism and the degree of tamoxifen
303 toxicity are greatly modulated by bacteria, where *B. subtilis* induces a non-apoptotic

304 mechanism that is three orders of magnitude more severe than apoptotic mechanism
305 elicited by tamoxifen in the presence of either *E. coli* or *C. aquatica* (**Figure 6**).
306 In the *C. elegans* model, bacteria form a source of nutrition, can be pathogenic,
307 and can inhabit the gut as the animal ages (Felix and Braendle, 2010). Both in the
308 laboratory and in the wild, the animals are constantly exposed to bacterial metabolism
309 which provides nutrients and contributes to animal physiology (Yilmaz and Walhout,
310 2014). Our findings illuminate the possible effects the microbiota may have on tamoxifen
311 off-target effect toxicity and the treatment of ER-independent malignancies (Clifford et al.,
312 2020). It is tempting to speculate that tamoxifen activity could be modulated by
313 perturbations of the microbiota using antibiotics or probiotics. Notably, *B. subtilis*, which
314 is present in a large proportion of commercially available probiotics (Joerger and Ganguly,
315 2017) may affect patients treated with tamoxifen. Our findings of the role of FA
316 metabolism and oxidative stress further suggest that studies of nutritional intake of fats
317 and vitamin E in humans may shed light on whether the off-target mechanisms discovered
318 herein are conserved.
319

320 **FA Modulation of Tamoxifen Toxicity**

321 We uncovered complex relationships between bacteria, host FA metabolism, apoptosis,
322 and tamoxifen toxicity. The literature about the relationship between FAs and cell survival
323 integrates two major components: distinct FA-species display different oxidation
324 potentials (Gardner, 1989), and different potentials to induce alternative cell-death
325 mechanisms (Garbarino and Sturley, 2009; Magtanong et al., 2019). Our data using
326 lipophilic ROS-scavenging vitamin E and apoptosis-deficient animals suggest that

327 tamoxifen-toxicity relies on these two entangled components. MUFAs are generally
328 described as 'healthy" FAs, as they buffer the oxidative stress of the ROS-sensitive
329 PUFAs (Magtanong et al., 2019). To our knowledge, there is only one report on the effects
330 of the MUFA cis-vaccenic acid, which found that cis-VA accumulation inhibits cell survival,
331 which is opposite to other MUFAs tested in parallel (Nakamura et al., 2018). Overall, the
332 literature is consistent with the observation of extreme tamoxifen toxicity in *B. subtilis*-fed
333 animals that do not provide the animal with MUFAs, and in *C. aquatica*-fed animals that
334 accumulate cis-vaccenic acid. Further studies are required to systematically determine
335 the effects of different FAs on cell survival and tamoxifen toxicity in human cells.

336

337 ***dhs-19:* a Potential Integrator of FA Metabolism and Oxidative Stress**

338 Knockdown of or mutations in *dhs-19* enhance tamoxifen toxicity in animals fed *E. coli*.
339 The precise molecular or metabolic function of DHS-19 is unknown. It encodes a
340 dehydrogenase and is a marker of lipid droplets (Zhang et al., 2012), which are essential
341 for FA homeostasis in all eukaryotes (Olzmann and Carvalho, 2019). Based on enzyme
342 homology, DHS-19 is predicted to act in retinoid metabolism, through the interconversion
343 of retinol and retinal (Walker et al., 2021). This reaction precedes the synthesis of retinyl
344 palmitate which consumes palmitoyl-CoA, which is a precursor for the synthesis of
345 palmitoleic and vaccenic acid, both of which potentiate tamoxifen toxicity in *C. elegans*
346 when animals are fed *E. coli*. Retinoids are also potent ROS scavengers and have been
347 shown to act synergically with vitamin E to reduce lipid oxidative stress (Tesoriere et al.,
348 1993). Together, this suggests that the increase in tamoxifen toxicity by *dhs-19*

349 perturbation could result from a complex integration of metabolic cues involving oxidative
350 stress and retinoid metabolism.
351

352 **You are What you Eat: *C. elegans* FA Composition is Determined by its Diet**

353 *C. elegans* is a remarkable animal with a fixed lineage in which wild type animals develop
354 deterministically to adults with precisely 959 somatic nuclei (Sulston and Horvitz, 1977;
355 Sulston et al., 1983). Therefore, one would assume that all adult animals are essentially
356 the same. Here we show that wild type animals can exhibit marked differences in their FA
357 composition, depending on which bacterial diet they are fed. To our knowledge,
358 *C. elegans* FA composition has only been studied in animals fed *E. coli*, and the profiles
359 observed in our experiments are consistent with the only available previous study (Brooks
360 et al., 2009). Here, we observe much more drastic changes in FA composition in animals
361 fed *C. aquatica* or *B. subtilis*, relative to those fed *E. coli*. First, the MUFA, mmBCFA or
362 CPFAs content of the animals strongly reflects the dietary input; a diet of *C. aquatica* is
363 rich in MUFAs, and a diet of *B. subtilis* is rich in mmBCFAs, and these FAs accumulate
364 in the animals. This result demonstrates that the animal's membranes are permissive to
365 varying levels of these types of FAs. In contrast, the PUFA composition of *C. elegans* is
366 largely independent of its bacterial diet. While PUFAs are essential dietary FAs in
367 humans, *C. elegans* synthesize PUFAs de novo (Watts and Browse, 2002). This result
368 indicates that *C. elegans* PUFA levels are sensed, and that metabolic fluxes in FA
369 biosynthesis pathways are adjusted to maintain relative levels in a tight regime. It is
370 therefore perhaps not surprising that PUFA deficiencies have been associated with
371 developmental and neuronal defects in *C. elegans* (Connor and Watts, 2019). Future

372 studies are required to reveal to what the extent wild type *C. elegans* exhibit other fitness
373 changes in response to differences in FA composition.
374
375 **Cell Death and Organismal Death**
376 How does cell-death connect to organism death? Fifty years after Horvitz and Sulston
377 first described apoptosis in *C. elegans* (Sulston and Horvitz, 1977), it remains unclear
378 how cell death mechanisms communicate and how they relate to organismal phenotypes
379 including death. Other open questions that remain to be answered are: What is the exact
380 nature of the triggers directing decisions in the induction of alternative cell-death
381 mechanisms? And how do bacteria affect cell-death potentials? This study provides a
382 foundation for future studies to address fundamental questions related to cell-death and
383 organismal fate.
384
385 **ACKNOWLEDGEMENTS**
386 We thank members of the Walhout lab and Job Dekker for discussion and critical reading
387 of the manuscript. This work was supported by grants from the National Institutes of
388 Health DK068429 and GM082971 to A.J.M.W., GM127559 to M.J.L., AG058950 to
389 C.O.P. and GM122393 to A.G.G. Several bacterial and nematode strains used in this
390 work were provided by the CGC, which is funded by the NIH Office of Research
391 Infrastructure Programs (P40 OD010440).
392
393 **AUTHOR CONTRIBUTIONS**

394 C.D., A.G.G. and A.J.M.W. conceived the study. C.D. and A.G.G. performed most
395 experiments with technical help from M.W., H.D., Y.R. and A.F.V. performed the fatty acid
396 measurements under supervision of C.P.O. H.N. engineered the Δ*dhs-19* mutant strain.
397 M.H. and C.D. performed the mammalian cell experiments under the supervision of M.L.
398 H.Z. and C.D. performed and analyzed the RNA-seq experiments. The manuscript was
399 written by C.D., and A.J.M.W. with editing by all other authors.
400

401 **DECLARATION OF INTERESTS**

402 All authors have no competing interests.
403

404 **FIGURE LEGENDS**

405 **Figure 1. Tamoxifen Kills ER-Negative Breast Cancer Cells and Animals**

406 (A, B) The growth rate index (A) and fractional viability (B) of ER-positive (T-47D) and
407 ER-negative (MDA-MB-231) breast cancer cells plotted as a function of increasing
408 concentrations of tamoxifen.

409 (C) Bright-field images showing *C. elegans* supplemented with increasing doses of
410 tamoxifen, fed *E. coli*, *C. aquatica*, and *B. subtilis*. Images were taken at 2x magnification
411 after 48h exposure to tamoxifen.

412 (D) Dose response curves of *C. elegans* supplemented with increasing doses of
413 tamoxifen, fed *E. coli*, *C. aquatica*, and *B. subtilis.* Data are represented as mean ±SEM
414 of three biological replicates.
415

416 **Figure 2. Host Long Chain Fatty Acid Synthesis Modulates Tamoxifen Toxicity**

417 (A) Screening a metabolic gene RNAi library identified three genes (*dhs-19*, *elo-3* and
418 *elo-5*) that, when knocked down, increase TAM toxicity. Animals were fed *E. coli* HT115
419 expressing double stranded RNA as indicated. Control indicates *E. coli* containing vector
420 control plasmid (pL4440). Bright-field images were taken at 2x magnification after a 48h
421 exposure to tamoxifen.
422 (B) Tamoxifen dose response curves comparing Δ*dhs-19* mutant animals to wild type
423 animals. See also **Figure S1**.
424 (C) *C. elegans* fatty acid biosynthesis pathway. Gene names are colored by enzymatic
425 function: FA elongation in blue, FA desaturation in pink, and acyl-CoA synthesis in purple.
426 (D) Cartoon illustrating calculation of differential area under curve (ΔAUC) used in panels
427 E and F. AUCs were calculated using average DRCs and statistical significance was
428 assessed by performing 2way anovas using Graphpad Prism (v9) on original DRCs and
429 are reported in **Table S1** and **S2**. See also **Figures S2** and **S3**.
430 (E, F) Bar graph showing ΔAUC values obtained from average full DRCs for animals
431 exposed to RNAi of indicated genes.
432
433 **Figure 3. Long Chain Fatty Acid Profiles of Bacteria and *C. elegans* Fed Different**
434 **Bacteria**
435 (A, B) Bubble plots showing long chain fatty acid proportions measured by GC-MS in the
436 indicated bacteria (A), and animals fed the indicated bacteria (B). Bubble sizes are
437 indicative of FA ratios within the sample of interest and are not indicative of absolute
438 quantities. Ratios are available in **Table S3** and **S4**. Data are represented as mean of

439 three to six biological replicates. Statistical pairwise comparisons are available in **Table**
440 **S5**.
441
442 **Figure 4. Long Chain Fatty Acid Supplementation Modulates Tamoxifen Toxicity**
443 (A-M) Unless otherwise indicated, fatty acids and vitamin E were supplemented to
444 bacterial culture medium, as described previously (Devkota et al., 2021).
445 (A-C) DRCs of tamoxifen toxicity with and without FA cocktail supplementation on animals
446 fed *E. coli* (A), *C. aquatica* (B) or *B. subtilis* (C).
447 (D,E) DRCs of of tamoxifen toxicity with and without PUFA (ALA) supplementation on
448 animals fed *E. coli* (D) or *C. aquatica* (E).
449 (F) Growth curves of *B. subtilis* supplemented with PUFAs ALA or GLA. For clarity, no
450 error bars are reported in the graph, n=3.
451 (G,H) DRCs of tamoxifen toxicity with and without MUFA (VA) supplementation on
452 animals fed *E. coli* (G) or *C. aquatica* (H).
453 (I) Growth curves of *B. subtilis* supplemented with MUFAs VA, PA, or OA. No error bars
454 are reported in the graph, n=3.
455 (J-L) DRCs of tamoxifen toxicity with and without vitamin E supplementation on animals
456 fed *E. coli* (J), *C. aquatica* (K) or *B. subtilis* (L).
457 (M) DRCs of tamoxifen toxicity with and without the antioxidants vitamin E and
458 N-acetyl-cysteine (NAC). Culture: NAC was supplemented in the bacterial culture medium
459 as for vitamin E. Medium: NAC was supplemented to the NGM.
460 DRC: dose response curve, FA: fatty acid, MUFA: mono-unsaturated FA,
461 PUFA: poly-unsaturated FA, ALA: alpha-linoleic acid, GLA: gamma-linoleic acid,

462 DGLA: di-homo-gamma-linoleic acid, VA: cis-vaccenic acid, PA: palmitoleic acid,
463 OA: oleic acid. Statistical analysis of DRCs was conducted by performing 2-way Anova
464 using GraphPad Prism (v9) and are reported in **Table S6**. Larger panel of fatty acid
465 supplements was tested in **Figure S5**.
466
467 **Figure 5. Bacteria Affect the Modulation of Tamoxifen Toxicity by Apoptosis**
468 (A) Bright-field images (left) and bar graph (right) of wild type and Δ*ced-3* animals fed
469 *E. coli*.
470 (B) Bright-field images (left) and bar graph (right) of wild type and Δ*ced-3* animals fed
471 *C. aquatica*.
472 (C) Bright-field images (left) and bar graph (right) of wild type and Δ*ced-3* animals fed
473 *B. subtilis*.
474 (D) Volcano plot distribution of genes which expression changed significantly in animals
475 fed *E. coli* and exposed to 400 μM tamoxifen (FDR<0.1, >2-fold change). Pink indicates
476 genes encoding enzymes participating in FA metabolism, and red indicates genes
477 encoding for enzymes that may be involved in the detoxification of tamoxifen.
478
479 **Figure 6. Model of Interplay Between Bacteria, Fatty Acid Metabolism, and Death**
480 **Pathways Affecting Tamoxifen Toxicity**
481
482 **STAR * METHODS**
483
484 **RESOURCE AVAILABILITY**

485 **Lead contact**

486 Further information and requests for reagents may be directed to, and will be fulfilled by
487 the corresponding author A.J.M. Walhout (marian.walhout@umassmed.edu).

488

489 **Materials availability**

490 All requests for resources and reagents should be directed to and will be fulfilled by the
491 Lead Contact. All reagents will be made available on request after completion of a
492 Materials Transfer Agreement.

493

494 **EXPERIMENTAL MODEL AND SUBJECT DETAILS**

495 ***C. elegans***

496 *C. elegans* N2 (Bristol) was used as the wild-type strain. Prior to all experiments, animals
497 were maintained on Nematode Growth Media (NGM) and fed a diet of *E. coli* OP50. The
498 *C. elegans ced-3(n717)* mutant strain was kindly provided by the Francis lab (UMass
499 Medical School) and was first described in (8598288). The *C. elegans dhs-19(VL1313)*
500 mutant strain was generated using CRISPR-Cas9 genome editing (Kim et al., 2014).

501

502 **Bacterial Strains**

503 *Escherichia coli* BW25113, *E. coli* HT115, *Comamonas aquatica* DA1877, and *Bacillus*
504 *subtilis* sp168 were grown in LB, overnight at 37°C to stationary phase under agitation
505 (200 rpm). The dietary effects on tamoxifen toxicity described herein were independent
506 of the *E. coli* strain tested. Experiments were conducted using *E. coli* BW25113, unless
507 stated otherwise.

508

509 **METHOD DETAILS**

510 **Chemotherapeutic Drugs containing NGM preparation**

511 Tamoxifen citrate (Selleckchem, S1972) was dissolved to 150 mM in sterile dimethyl
512 sulfoxide (DMSO), aliquoted and stored at -20°C. Stock solutions were diluted in series
513 to 200X the final concentration and added at a final volume of 0.5% to NGM agar heated
514 to 55°C. Drug containing NGM plates were dried overnight at room temperature. NGM
515 was supplemented with antibiotics for experiments in 96-well plate format, and 2 mM
516 IPTG for RNAi experiments. 96-well and 48-well plates were seeded with 15 µL and 30
517 µL of bacterial cultures, respectively. Plates were then dried for 6h at room temperature
518 and kept overnight at room temperature before being used. *E. coli* cultures were
519 concentrated 1-2X, and *C. aquatica* DA1877 and *B. subtilis* sp168 strains were
520 concentrated 2-4X prior to seeding onto NGM agar plates, to normalize for post-seeding
521 bacterial growth.

522

523 **RNAi screen**

524 We tested a collection of 1,645 individual *E. coli* HT115 strains expressing dsRNA against
525 a unique *C. elegans* metabolic gene, and originating from the ORFeome (Rual et al.,
526 2004) or the Ahringer (Kamath et al., 2003) libraries. The screens were performed using
527 96-well plates containing NGM supplemented with tamoxifen, 50 µg/mL ampicillin, and 2
528 mM IPTG. We used a low dose of 300 µM tamoxifen to identify knockdowns that
529 aggravate tamoxifen toxicity, and a high dose of 600 µM tamoxifen identify knockdowns
530 that mitigate tamoxifen toxicity. Approximatively 20 L1-arrested animals were added to

531 each well. Two days later, hits were scored visually using a dissecting microscope as
532 knockdowns leading to a difference in animal drug response relative to animals fed an
533 *E. coli* strain containing the empty dsRNA vector backbone (pL4440).
534
535 ***C. elegans* Dose-Response Curves**
536 Dose-response curves (DRCs) were performed in 48-well plates with six to twelve
537 technical replicates. Fifty to one hundred L1-arrested animals were plated onto each well
538 and incubated at 20°C for 48 hours. Animals that developed beyond the L1 stage were
539 counted under a dissecting microscope. The percentage of animals that did not
540 developed was calculated relative to the total number of animals developed in the control
541 condition. For ΔAUCs in Figures 3D-F, we used the average AUCs from the DRCs of the
542 *E. coli* BW25113 and *E. coli* HT115 pL4440 control conditions.
543
544 **Bacterial Growth Curves**
545 Bacteria were first grown overnight in LB at 37°C and shaking at 200 rpm. Next, bacterial
546 cultures were diluted 1:200 and grown in LB supplemented with 1% of FA supplements
547 (or ethanol vehicle as a control). Cultures were then grown for 20h at 37°C and shaking
548 at 200 rpm, in an Eon™ Microplate Spectrophotometer (BioTek) and absorbance at 600
549 nm was measured every 900 s.
550
551 **Fatty Acid and Vitamin E supplementations**
552 Undiluted fatty acid cocktail and PUFAs solutions were supplemented at 1% v.v. in LB for
553 overnight growth. MUFAs were first diluted 1:10 in ethanol and supplemented at 1% v.v.

554 in LB for overnight growth. Undiluted vitamin E was supplemented from 0.1% to 10% in
555 LB for overnight growth.
556
557 ***C. elegans* FA Measurements**
558 Fatty acid measurements in bacteria and animals were performed as described before
559 (Perez and Van Gilst, 2008). Briefly, lipids were extracted from whole animals using a 2:1
560 chloroform:methanol mixture and dried in liquid nitrogen. A calibrated phospholipid or
561 triacylglycerol standard was added to the extracted lipids before separation by
562 solid-phase exchange chromatography. Purified lipids were then converted into fatty acid
563 methyl esters by incubation with methanol/2.5% H_2SO_4 before GC/MS analysis. All data
564 are presented as percentage of the total fraction of fatty acids measured in the sample.
565
566 **Mammalian Cell Culture**
567 MDA-MB-231 cells were obtained from the American Type Culture Collection (ATCC,
568 Manassas, VA) and cultured in Dulbecco's modified Eagle's medium
569 (Corning, 10-017-CV). T-47D cells were grown in RPMI-1640 media (Gibco, 11875119).
570 All cell culture media were supplemented with 10% FBS (Hyclone, SH30910.03, lot
571 AYG161519), 2 mM glutamine (Corning, 25-005-CI), and penicillin/streptomycin
572 (Corning, 30-002-CI). Cells were cultured in a humidified incubator at 37°C with 5% CO_2.
573 In addition, cell lines were maintained at low passage numbers and regularly tested for
574 mycoplasma.
575
576 **Mammalian Drug Sensitivity Assays**

577 Measurement of lethal fraction (LF), fractional viability (FV), and normalized growth rate
578 inhibition (GR) were performed using the FLICK assay as previously described (Richards
579 et al., 2021). Briefly, cells were seeded in 96-well optical-bottom black-walled plates
580 (Greiner Bio-One, 655090) in 90 µL of media and allowed to adhere overnight. Density
581 was optimized for each cell line depending on the growth rate of the cells and the duration
582 of the assay. Dilutions of tamoxifen (Selleckchem, S1972) were prepared at 10x final
583 concentration in media containing 50 µM SYTOX green (Thermo Fisher Scientific,
584 S7020). 10 µL of drug combinations were supplemented to the cell culture media and
585 fluorescence signals (excitation = 504 nm, emission = 523 nm) were recorded at the
586 indicated time points on a Tecan Spark multimode plate reader. Total cell fluorescence
587 was evaluated by lysing untreated cells at the start and experimental conditions at the
588 end of the assay, using a supplement of 0.1% Triton X-100 (Fisher Scientific, BP151-500)
589 diluted in PBS.
590
591 **Gene expression profiling by RNA-seq**
592 Total RNA was extracted using TRIzol (ThermoFisher), followed by DNase I (NEB)
593 treatment and purified using the Direct-zol RNA mini-prep kit (Zymo research). RNA
594 quality was verified by agarose gel electrophoresis. Briefly, multiplexed libraries were
595 prepared using Cel-seq2 (Hashimshony et al., 2016). Two to three biological replicates
596 were sequenced with a NextSeq 500/550 High Output Kit v2.5 (75 Cycles) on a
597 Nextseq500 sequencer. Paired end sequencing was performed; 13 cycles for read 1, six
598 cycles for the illumina index and 73 cycles for read 2. Analysis were performed as

599 previously detailed (Giese et al., 2020), using a homemade DolphinNext pipeline
600 (Yukselen et al., 2020).
601

602 **DATA AND CODE AVAILABILITY**

603 RNA-seq data have been deposited at GEO.

604 This study does not report original code.

605

606 **SUPPLEMENTAL INFORMATION**

607 Supplemental information includes five Supplemental Figures and six Supplemental
608 Tables.

609

610 **REFERENCES**

611 Bekele, R.T., Venkatraman, G., Liu, R.Z., Tang, X., Mi, S., Benesch, M.G., Mackey, J.R., Godbout, R.,
612 Curtis, J.M., McMullen, T.P.*, et al.* (2016). Oxidative stress contributes to the tamoxifen-induced killing of
613 breast cancer cells: implications for tamoxifen therapy and resistance. Sci Rep *6*, 21164.
614
615 Brooks, K.K., Liang, B., and Watts, J.L. (2009). The influence of bacterial diet on fat storage in *C. elegans.*
616 PLoS One *4*, e7545.
617
618 Clifford, R.E., Bowden, D., Blower, E., Kirwan, C.C., and Vimalachandran, D. (2020). Does tamoxifen have
619 a therapeutic role outside of breast cancer? A systematic review of the evidence. Surg Oncol *33*, 100-107.
620
621 Connor, A.J., and Watts, J.L. (2019). Omega-3 and omega-6 fatty acid metabolism: modeling growth and
622 disease uisng *Caenorhabditis elegans*. In Omega fatty acids in brain and neurological health (second
623 edition) (Academic Press), pp. 107-116.
624
625 Dancy, B.C., Chen, S.W., Drechsler, R., Gafken, P.R., and Olsen, C.P. (2015). 13C- and 15N-Labeling
626 Strategies Combined with Mass Spectrometry Comprehensively Quantify Phospholipid Dynamics in *C.*
627 *elegans*. PLoS One *10*, e0141850.
628
629 Devkota, R., Kaper, D., Bodhicharla, R., Henricsson, M., Boren, J., and Pilon, M. (2021). A Genetic Titration
630 of Membrane Composition in *C. elegans* Reveals its Importance for Multiple Cellular and Physiological
631 Traits. Genetics.
632
633 Diot, C., Garcia-Gonzalez, A.P., and Walhout, A.J.M. (2018). *C. elegans* and its bacterial diet: an
634 interspecies model to explore the effects of microbiota on drug response. Drug Discovery Today: Disease
635 Models *28*, 21-26.
636

637
638 Felix, M.A., and Braendle, C. (2010). The natural history of *Caenorhabditis elegans*. Curr Biol *20*, R965-
639 969.
640
641 Galluzzi, L., Vitale, I., Aaronson, S.A., Abrams, J.M., Adam, D., Agostinis, P., Alnemri, E.S., Altucci, L.,
642 Amelio, I., Andrews, D.W.*, et al.* (2018). Molecular mechanisms of cell death: recommendations of the
643 Nomenclature Committee on Cell Death 2018. Cell Death Differ *25*, 486-541.
644
645 Garbarino, J., and Sturley, S.L. (2009). Saturated with fat: new perspectives on lipotoxicity. Curr Opin Clin
646 Nutr Metab Care *12*, 110-116.
647
648 Garcia-Gonzalez, A.P., Ritter, A.D., Shrestha, S., Andersen, E.C., Yilmaz, L.S., and Walhout, A.J.M. (2017).
649 Bacterial metabolism affects the *C. elegans* response to cancer chemotherapeutics. Cell *169*, 431-441
650 e438.
651
652 Garcia-Gonzalez, A.P., and Walhout, A.J.M. (2017). Worms, bugs and drugs: *Caenorhabditis elegans* as a
653 model for host-microbe-drug interactions. Curr Opin Systems Biol *6*, 46-50.
654
655 Gardner, H.W. (1989). Oxygen radical chemistry of polyunsaturated fatty acids. Free Radic Biol Med *7*, 65-
656 86.
657
658 Giese, G.E., Walker, M.D., Ponomarova, O., Zhang, H., Li, X., Minevich, G., and Walhout, A.J. (2020). *C.*
659 *elegans* methionine/S-adenosylmethionine cycle activity is sensed and adjusted by a nuclear hormone
660 receptor. Elife *9*.
661
662 Hafner, M., Niepel, M., Chung, M., and Sorger, P.K. (2016). Growth rate inhibition metrics correct for
663 confounders in measuring sensitivity to cancer drugs. Nat Methods *13*, 521-527.
664
665 Hashimshony, T., Senderovich, N., Avital, G., Klochendler, A., de Leeuw, Y., Anavy, L., Gennert, D., Li, S.,
666 Livak, K.J., Rozenblatt-Rosen, O.*, et al.* (2016). CEL-Seq2: sensitive highly-multiplexed single-cell RNA-
667 Seq. Genome Biol *17*, 77.
668
669 Hrycay, E.G., and Bandiera, S.M. (2015). Involvement of Cytochrome P450 in Reactive Oxygen Species
670 Formation and Cancer. Adv Pharmacol *74*, 35-84.
671
672 Joerger, R.D., and Ganguly, A. (2017). Current Status of the Preharvest Application of Pro- and Prebiotics
673 to Farm Animals to Enhance the Microbial Safety of Animal Products. Microbiol Spectr *5*.
674
675 Jordan, V.C. (2003). Tamoxifen: a most unlikely pioneering medicine. Nat Rev Drug Discov *2*, 205-213.
676
677 Kamath, R.S., Fraser, A.G., Dong, Y., Poulin, G., Durbin, R., Gotta, M., Kanapin, A., Le Bot, N., Moreno,
678 S., Sohrmann, M.*, et al.* (2003). Systematic functional analysis of the *Caenorhabditis elegans* genome using
679 RNAi. Nature *421*, 231-237.
680
681 Kaneda, T. (1977). Fatty acids of the genus Bacillus: an example of branched-chain preference. Bacteriol
682 Rev *41*, 391-418.
683
684 Kim, H., Ishidate, T., Ghanta, K.S., Seth, M., Conte, D., Jr., Shirayama, M., and Mello, C.C. (2014). A co-
685 CRISPR strategy for efficient genome editing in *Caenorhabditis elegans*. Genetics *197*, 1069-1080.
686
687 Kisanga, E.R., Gjerde, J., Guerrieri-Gonzaga, A., Pigatto, F., Pesci-Feltri, A., Robertson, C., Serrano, D.,
688 Pelosi, G., Decensi, A., and Lien, E.A. (2004). Tamoxifen and metabolite concentrations in serum and
689 breast cancer tissue during three dose regimens in a randomized preoperative trial. Clin Cancer Res *10*,
690 2336-2343.
691

692 Koppel, N., Maini Rekdal, V., and Balskus, E.P. (2017). Chemical transformation of xenobiotics by the
693 human gut microbiota. Science *356*.
694
695 Lacroix, M., and Leclercq, G. (2004). Relevance of breast cancer cell lines as models for breast tumours:
696 an update. Breast Cancer Res Treat *83*, 249-289.
697
698 Liu, Y., Xu, S., Zhang, C., Zhu, X., Hammad, M.A., Zhang, X., Christian, M., Zhang, H., and Liu, P. (2018).
699 Hydroxysteroid dehydrogenase family proteins on lipid droplets through bacteria, *C. elegans*, and
700 mammals. Biochim Biophys Acta Mol Cell Biol Lipids *1863*, 881-894.
701
702 Magtanong, L., Ko, P.J., To, M., Cao, J.Y., Forcina, G.C., Tarangelo, A., Ward, C.C., Cho, K., Patti, G.J.,
703 Nomura, D.K.*, et al.* (2019). Exogenous Monounsaturated Fatty Acids Promote a Ferroptosis-Resistant Cell
704 State. Cell Chem Biol *26*, 420-432 e429.
705
706 Maier, L., Pruteanu, M., Kuhn, M., Zeller, G., Telzerow, A., Anderson, E.E., Brochado, A.R., Fernandez,
707 K.C., Dose, H., Mori, H.*, et al.* (2018). Extensive impact of non-antibiotic drugs on human gut bacteria.
708 Nature *555*, 623-628.
709
710 Manna, S., and Holz, M.K. (2016). Tamoxifen Action in ER-Negative Breast Cancer. Sign Transduct
711 Insights *5*, 1-7.
712
713 Nakamura, Y., Matsuzaka, T., Tahara-Hanaoka, S., Shibuya, K., Shimano, H., Nakahashi-Oda, C., and
714 Shibuya, A. (2018). Elovl6 regulates mechanical damage-induced keratinocyte death and skin
715 inflammation. Cell Death Dis *9*, 1181.
716
717 Olzmann, J.A., and Carvalho, P. (2019). Dynamics and functions of lipid droplets. Nat Rev Mol Cell Biol *20*,
718 137-155.
719
720 Perez, C.L., and Van Gilst, M.R. (2008). A 13C isotope labeling strategy reveals the influence of insulin
721 signaling on lipogenesis in *C. elegans*. Cell Metab *8*, 266-274.
722
723 Perez, M.A., Magtanong, L., Dixon, S.J., and Watts, J.L. (2020). Dietary Lipids Induce Ferroptosis in
724 *Caenorhabditis elegans* and Human Cancer Cells. Dev Cell *54*, 447-454 e444.
725
726 Reece-Hoyes, J.S., Deplancke, B., Shingles, J., Grove, C.A., Hope, I.A., and Walhout, A.J.M. (2005). A
727 compendium of *C. elegans* regulatory transcription factors: a resource for mapping transcription regulatory
728 networks. Genome Biol *6*, R110.
729
730 Richards, R., Honeywell, M.E., and Lee, M.J. (2021). FLICK: an optimized plate reader-based assay to
731 infer cell death kinetics. STAR Protoc *2*, 100327.
732
733 Robinson, S.P., Langan-Fahey, S.M., Johnson, D.A., and Jordan, V.C. (1991). Metabolites,
734 pharmacodynamics, and pharmacokinetics of tamoxifen in rats and mice compared to the breast cancer
735 patient. Drug Metab Dispos *19*, 36-43.
736
737 Rosener, B., Sayin, S., Oluoch, P.O., Garcia Gonzalez, A.P., Mori, H., Walhout, A.J., and Mitchell, A.
738 (2020). Evolved bacterial resistance against fluoropyrimidines can lower chemotherapy impact in the
739 *Caenorhabditis elegans* host. Elife *9*.
740
741 Rual, J.-F., Ceron, J., Koreth, J., Hao, T., Nicot, A.-S., Hirozane-Kishikawa, T., Vandenhaute, J., Orkin,
742 S.H., Hill, D.E., van den Heuvel, S.*, et al.* (2004). Toward improving *Caenorhabditis elegans* phenome
743 mapping with an ORFeome-based RNAi library. Genome Res *14*, 2162-2168.
744
745 Schwartz, H.R., Richards, R., Fontana, R.E., Joyce, A.J., Honeywell, M.E., and Lee, M.J. (2020). Drug
746 GRADE: An Integrated Analysis of Population Growth and Cell Death Reveals Drug-Specific and Cancer
747 Subtype-Specific Response Profiles. Cell Rep *31*, 107800.

748
749 Scott, T.A., Quintaneiro, L.M., Norvaisas, P., Lui, P.P., Wilson, M.P., Leung, K.Y., Herrera-Dominguez, L.,
750 Sudiwala, S., Pessia, A., Clayton, P.T.*, et al.* (2017). Host-microbe co-metabolism cictates cancer drug
751 efficacy in *C. elegans*. Cell *169*, 442-456 e418.
752
753 Selwyn, F.P., Cui, J.Y., and Klaassen, C.D. (2015). RNA-Seq Quantification of Hepatic Drug Processing
754 Genes in Germ-Free Mice. Drug Metab Dispos *43*, 1572-1580.
755
756 Shagufta, and Ahmad, I. (2018). Tamoxifen a pioneering drug: An update on the therapeutic potential of
757 tamoxifen derivatives. Eur J Med Chem *143*, 515-531.
758
759 Sharma, S., Morinaga, H., Hwang, V., Fan, W., Fernandez, M.O., Varki, N., Olefsky, J.M., and Webster,
760 N.J. (2013). Free fatty acids induce Lhb mRNA but suppress Fshb mRNA in pituitary LbetaT2 gonadotropes
761 and diet-induced obesity reduces FSH levels in male mice and disrupts the proestrous LH/FSH surge in
762 female mice. Endocrinology *154*, 2188-2199.
763
764 Shelly, W., Draper, M.W., Krishnan, V., Wong, M., and Jaffe, R.B. (2008). Selective estrogen receptor
765 modulators: an update on recent clinical findings. Obstet Gynecol Surv *63*, 163-181.
766
767 Singh, M.S., Francis, P.A., and Michael, M. (2011). Tamoxifen, cytochrome P450 genes and breast cancer
768 clinical outcomes. Breast *20*, 111-118.
769
770 Sivik, T., Gunnarsson, C., Fornander, T., Nordenskjold, B., Skoog, L., Stal, O., and Jansson, A. (2012).
771 17beta-Hydroxysteroid dehydrogenase type 14 is a predictive marker for tamoxifen response in oestrogen
772 receptor positive breast cancer. PLoS One *7*, e40568.
773
774 Spanogiannopoulos, P., Bess, E.N., Carmody, R.N., and Turnbaugh, P.J. (2016). The microbial
775 pharmacists within us: a metagenomic view of xenobiotic metabolism. Nat Rev Microbiol *14*, 273-287.
776
777 Sulston, J.E., and Horvitz, H.R. (1977). Post-embryonic cell lineages of the nematode, *Caenorhabditis*
778 *elegans*. Dev Biol *56*, 110-156.
779
780 Sulston, J.E., Schierenberg, E., White, J.G., and Thomson, J.N. (1983). The embryonic cell lineage of the
781 nematode *Caenorhabditis elegans*. Dev Biol *100*, 64-119.
782
783 Taubert, S., Ward, J.D., and Yamamoto, K.R. (2011). Nuclear hormone receptors in nematodes: evolution
784 and function. Mol Cell Endocrinol *334*, 49-55.
785
786 Tesoriere, L., Ciaccio, M., Bongiorno, A., Riccio, A., Pintaudi, A.M., and Livrea, M.A. (1993). Antioxidant
787 activity of all-trans-retinol in homogeneous solution and in phosphatidylcholine liposomes. Arch Biochem
788 Biophys *307*, 217-223.
789
790 Traber, M.G., and Atkinson, J. (2007). Vitamin E, antioxidant and nothing more. Free Radic Biol Med *43*,
791 4-15.
792 Walker, M.D., Giese, G.E., Holdorf, A.D., Bhattacharya, S., Diot, C., Garcia-Gonzalez, A.P., Horowitz, B.,
793 Lee, Y.U., Leland, T., Li, X.*, et al.* (2021). WormPaths: *Caenorhabditis elegans* metabolic pathway
794 annotation and visualization. bioRxiv.
795
796 Watson, E., MacNeil, L.T., Arda, H.E., Zhu, L.J., and Walhout, A.J.M. (2013). Integration of metabolic and
797 gene regulatory networks modulates the *C. elegans* dietary response. Cell *153*, 253-266.
798
799 Watson, E., MacNeil, L.T., Ritter, A.D., Yilmaz, L.S., Rosebrock, A.P., Caudy, A.A., and Walhout, A.J.M.
800 (2014). Interspecies systems biology uncovers metabolites affecting *C. elegans* gene expression and life
801 history traits. Cell *156*, 759-770.
802

Watts, J.L. (2009). Fat synthesis and adiposity regulation in *Caenorhabditis elegans*. Trends Endocrinol Metab *20*, 58-65.

Watts, J.L., and Browse, J. (2002). Genetic dissection of polyunsaturated fatty acid synthesis in Caenorhabditis elegans. Proc Natl Acad Sci U S A *99*, 5854-5859.

Yilmaz, L.S., Li, X., Nanda, S., Fox, B., Schroeder, F., and Walhout, A.J. (2020). Modeling tissue-relevant *Caenorhabditis elegans* metabolism at network, pathway, reaction, and metabolite levels. Mol Syst Biol *16*, e9649.

Yilmaz, L.S., and Walhout, A.J. (2016). A *Caenorhabditis elegans g*enome-scale metabolic network model. Cell Syst *2*, 297-311.

Yilmaz, L.S., and Walhout, A.J.M. (2014). Worms, bacteria and micronutrients: an elegant model of our diet. Trends Genet *30*, 496-503.

Yuan, J., Shaham, S., Ledoux, S., Ellis, H.M., and Horvitz, H.R. (1993). The *C. elegans* cell death gene *ced-3* encodes a protein similar to mammalian interleukin-1 beta-converting enzyme. Cell *75*, 641-652.

Yukselen, O., Turkyilmaz, O., Ozturk, A.R., Garber, M., and Kucukural, A. (2020). DolphinNext: a distributed data processing platform for high throughput genomics. BMC Genomics *21*, 310.

Zhang, J., Li, X., Olmedo, M., Holdorf, A.D., Shang, Y., Artal-Sanz, M., Yilmaz, L.S., and Walhout, A.J.M. (2019). A delicate balance between bacterial iron and reactive oxygen species supports optimal *C. elegans* development. Cell Host Microbe *26*, 400-411 e403.

Zhang, P., Na, H., Liu, Z., Zhang, S., Xue, P., Chen, Y., Pu, J., Peng, G., Huang, X., Yang, F.*, et al.* (2012). Proteomic study and marker protein identification of *Caenorhabditis elegans* lipid droplets. Mol Cell Proteomics *11*, 317-328.

Zhang, X., Han, Y., Huang, W., Jin, M., and Gao, Z. (2021). The influence of the gut microbiota on the bioavailability of oral drugs. Acta Pharm Sin B *11*, 1789-1812.

Diot, *et al.* Figure 1

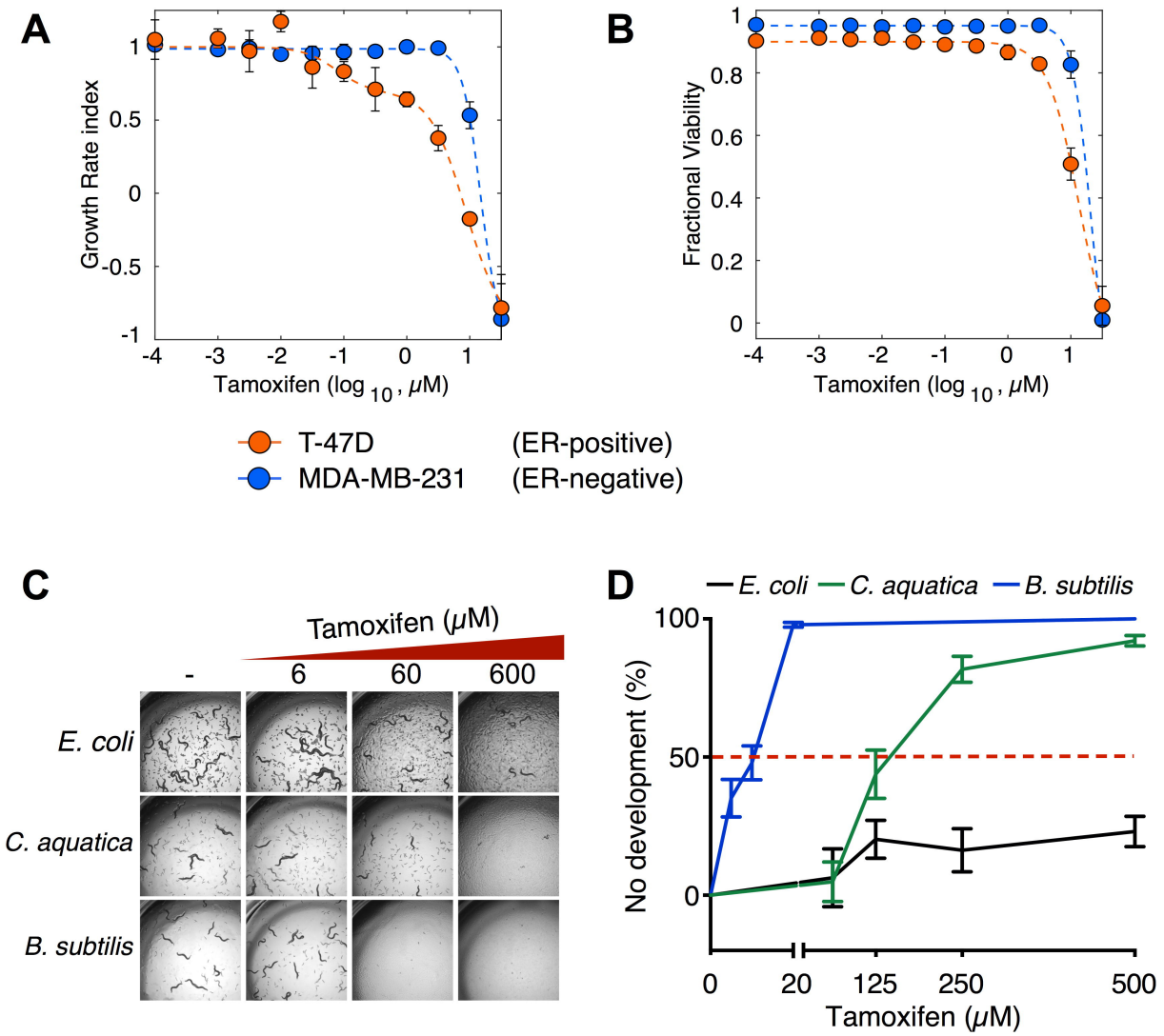

Diot *et al.* Figure 2

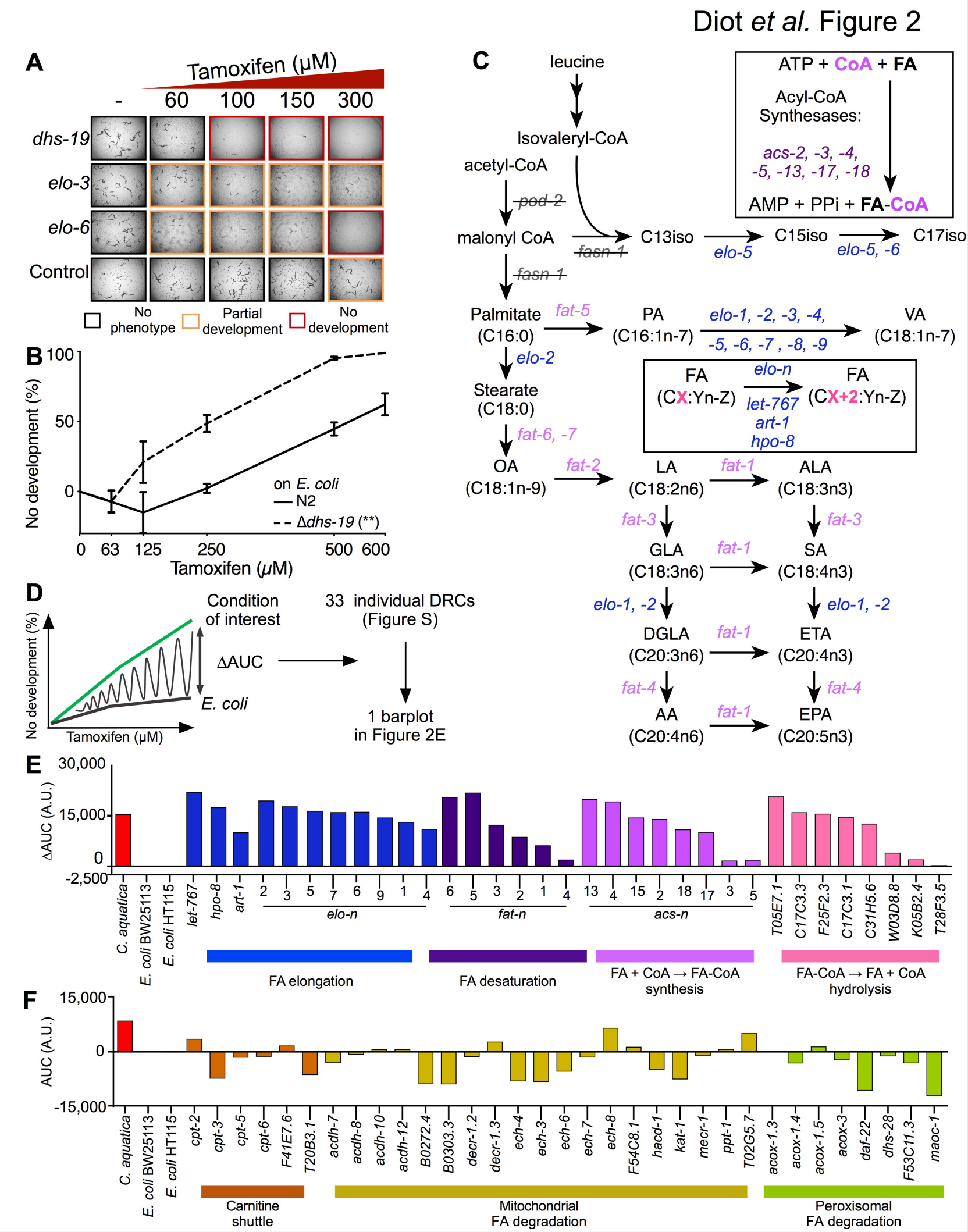

Diot, *et al.* Figure 3

Diot, *et al.* Figure 4

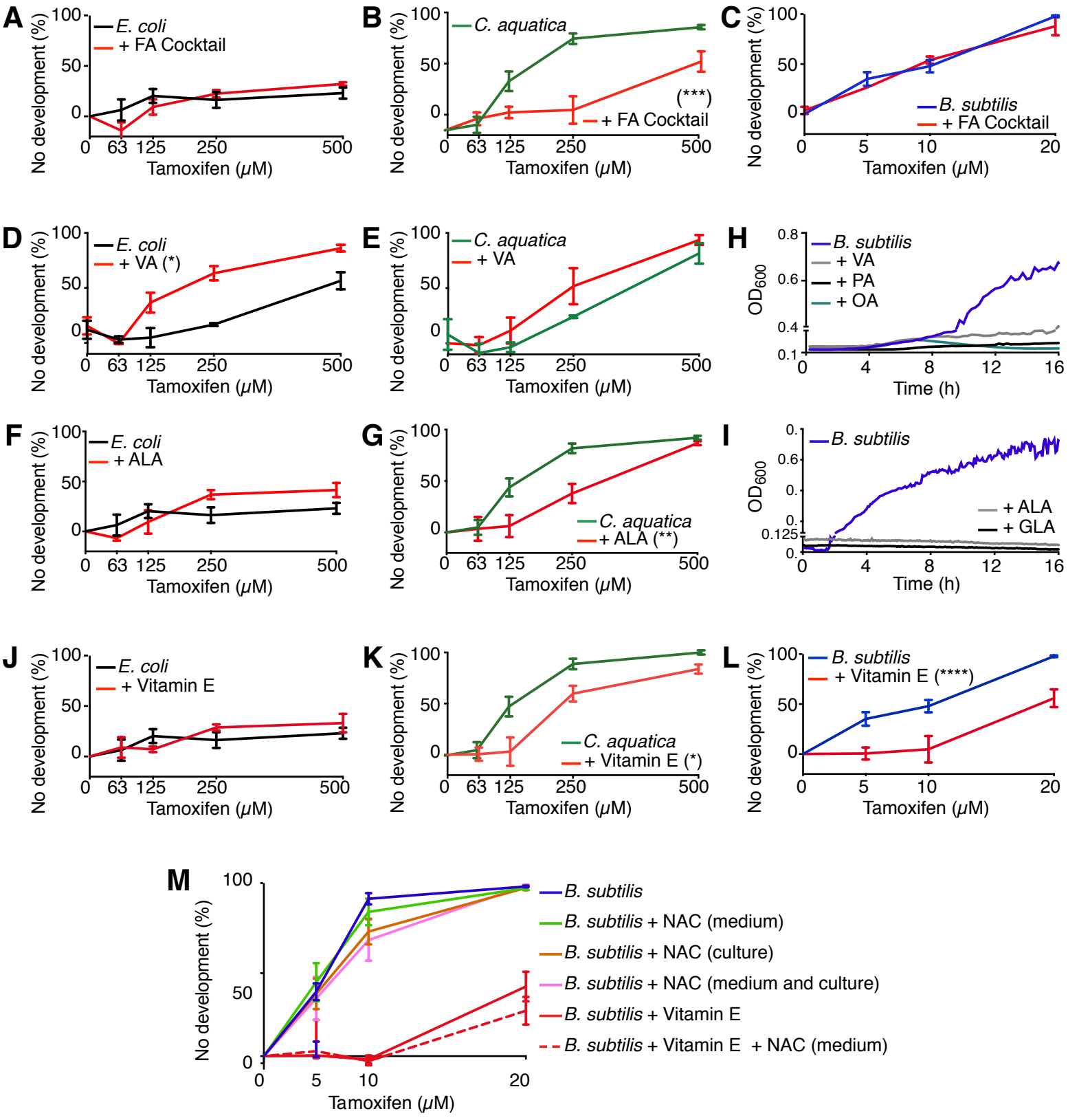

Diot, *et al.* Figure 5

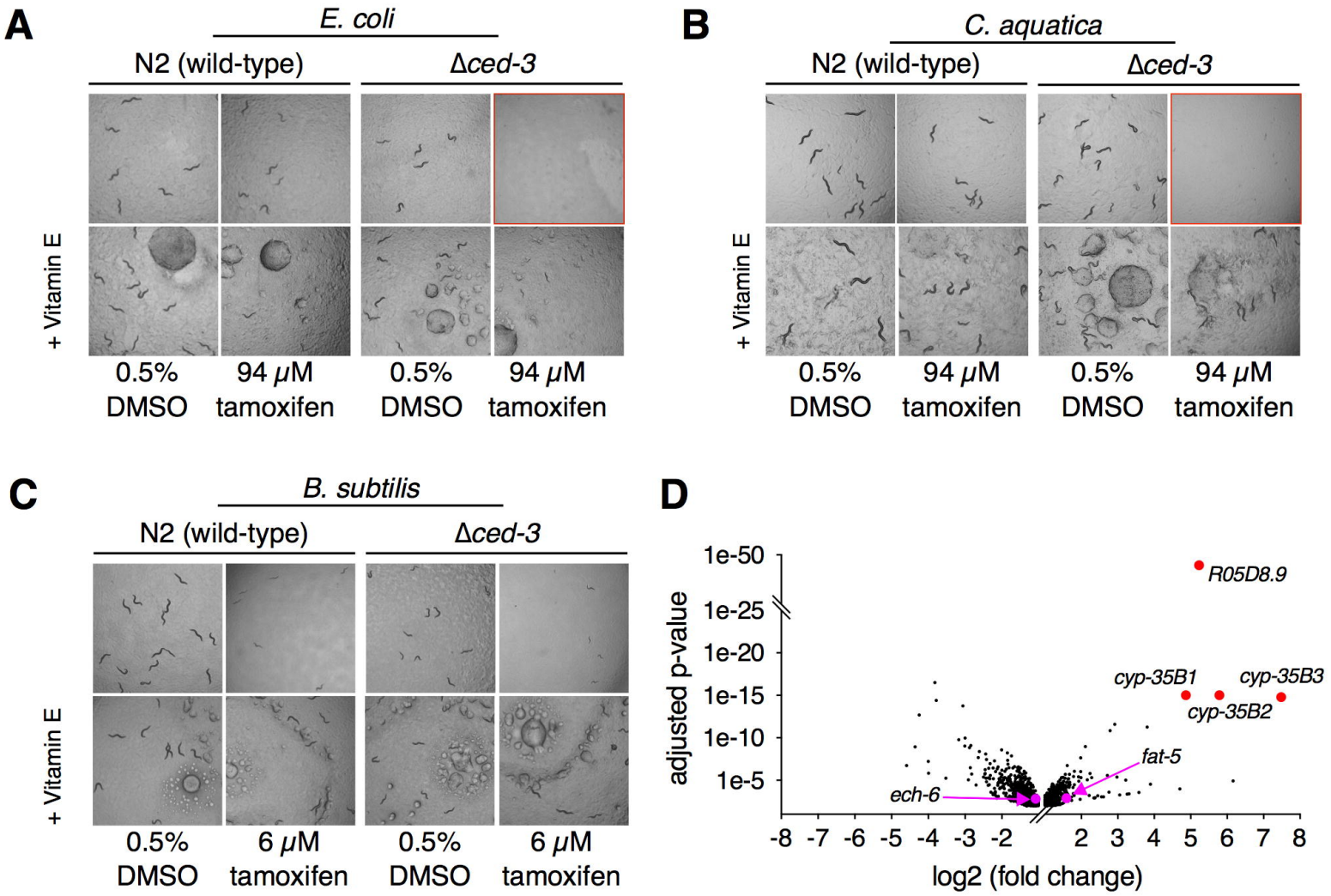
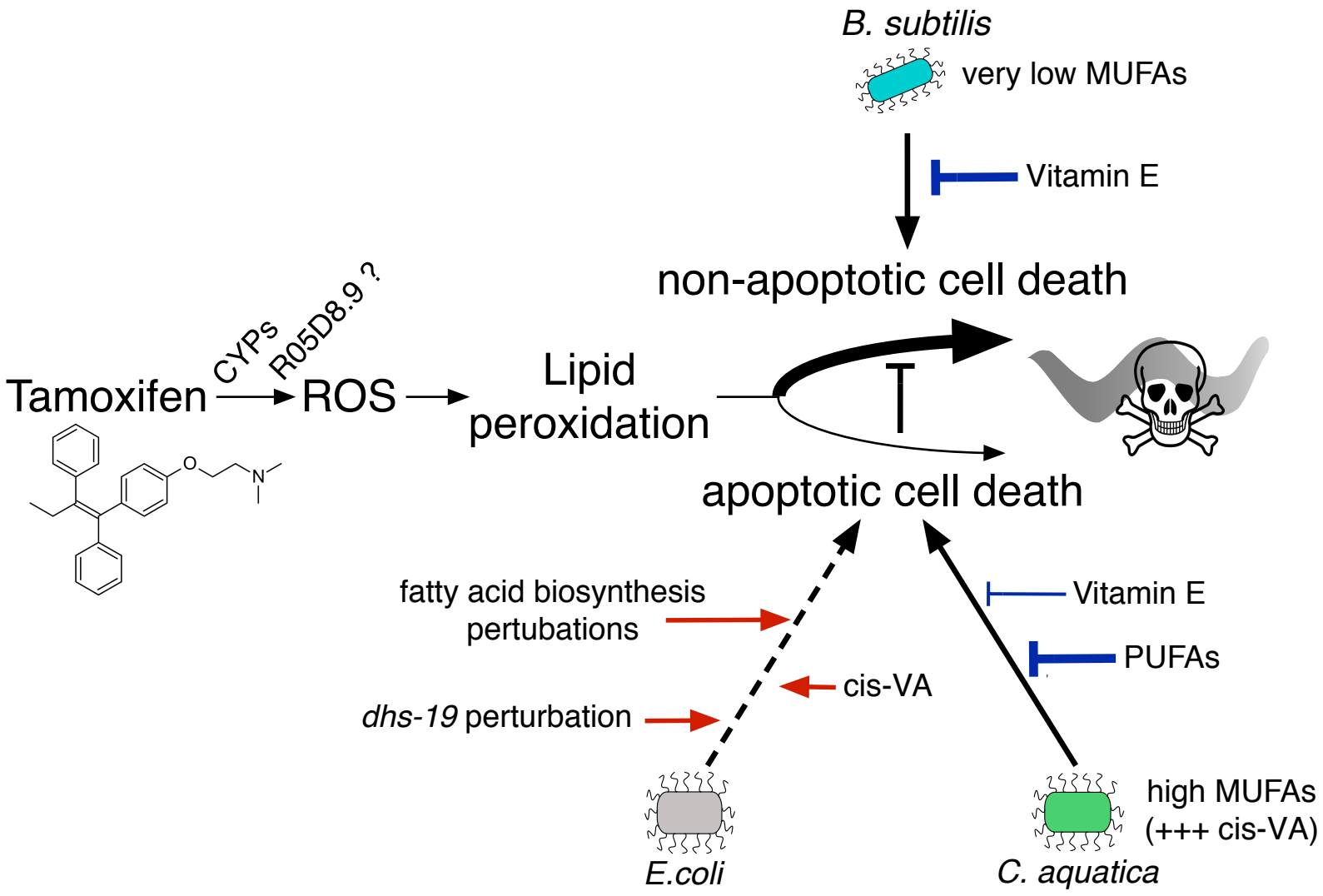
Diot *et al.* Figure 6